BeamMaP: Beamforming-based Machine Learning for Positioning in Massive MIMO Systems

Chong Liu, Hermann J. Helgert

School of Engineering and Applied Science, The George Washington University,
Washington, DC 20052
Email: cliu15@gwu.edu, hhelgert@gwu.edu

Abstract—**Existing positioning techniques can mostly overcome problems caused by path loss, background noise and Doppler effects, but multiple paths in complex indoor or outdoor environments present additional challenges. In this paper, we propose *BeamMaP* that can instantaneously locate users after training input data and steer the beams efficiently in a distributed massive Multiple-Input Multiple-Output (MIMO) system. To simulate a realistic environment, we evaluate the positioning accuracy with channel fingerprints collected from uplink Received Signal Strength (RSS) data, including Line-of-Sight (LoS) and Non-Line-of-Sight (NLoS), in the training data sets. Based on the adaptive beamforming, we employ the Rice distribution to sample the current mobile users locations in the testing data sets. Our simulation results achieve Reduced Root-Mean-Squared Estimation Error (RMSE) performance with increasing volume of training data. We prove our proposed model is more efficiency and steady in the positioning system compared with kNN and SVM. The results also demonstrate the effectiveness of the adaptive beamforming model in the testing process.**

Keywords–outdoor localization; machine learning; data training; beamforming.

I. INTRODUCTION

The future developing technologies, such as autonomous vehicles, Virtual Reality (VR) and the Internet of Things (IoT), are relying on more efficient bandwidth distribution and higher speed transmission [1] [2] [3] [4]. The next generation of wireless networks 5G should provide more accurate localization of the connected mobile devices and distribute the limited bandwidth in a more efficient way. Some new technologies employed in localization, especially including the massive Multiple-Input Multiple-Output (MIMO) and beamforming technologies, are explored in the 5G system [5]. The innovative design of massive MIMO disclosed in some publications utilizes a large number of upgraded array antennas (more than one hundred) to multiplex messages for several devices simultaneously. This component, implemented in future Base Stations (BSs), has been shown to play an essential role in positioning of Mobile Users (MUs) in cellular networks, including increased spectral efficiency, improved spatial diversity, and low complexity [6]. More importantly, a distributed design for massive MIMO is beneficial for positioning due to the better spatial diversity, which will be employed in this paper. Some proposed solutions applying the MIMO positioning techniques are mainly focused on the received signal information from the users, such as the Angle-of-Arrival (AoA), Time-of-Arrival (ToA), and Received Signal Strength (RSS) [7] [8] [9]. These features, singly or in combination, can be used in the localization of mobile users in indoor or outdoor environments.

Even though positioning in cellular networks widely uses the Global Positioning System (GPS) in urban or rural areas, the method becomes unreliable when the Line-of-Sight (LoS) and Non-Line-of-Sight (NLoS) are difficult to distinguish, such as in highly cluttered multipath scenarios (tens meters error) [10]. In some conventional method using the two-step localization techniques, the received LoS signals are processed at different base stations and AoA and/or ToA of each user can be obtained. Then the position of the user can be found by triangulation calculation [8]. However, the LoS path may be damped or obstructed, leading to large positioning errors, as is often the case in complex scenarios. Also, [8] is exploiting channel properties to distinguish LoS from NLoS signal paths, resulting in an improvement of performance. However, a large data gain with a combination of LoS and NLoS signal paths will require high computational complexity.

A. Related work

Big data collections combined with machine learning methods have been mentioned in solving the MUs localization in some of the literature [9] [11] [12]. For example, through collecting RSS, AoA and/or ToA, we typically provide efficient supervised or unsupervised techniques to estimate the coordinates of MUs. Some unsupervised methods, such as k-Nearest Neighbors (kNN), assume that there are many reference users at which vectors of RSS are obtained, and the target MU can be located as a weighted average of the closest k reference positions [11]. Although kNN is able to provide good performance in uniformly distributed references, we have to choose a better regression under the different k dimension, which will generate the large number of input training data and cause higher computational complexity. Additionally, supported machine learning methods, such as Support Vector Machines (SVM) [12] and deep learning methods [9], are explored to predict the coordinates of MUs after collecting amounts of RSSs and/or AoAs through different base stations. However, the method in [9] [12] will cause the estimation to be degraded when the number of MUs increases and interference between cells in the cellular networks becomes dramatically higher.

Based on the features of raw data sets, such as RSS mentioned below in the system, we employ a Gaussian Process Regression (GPR) model to estimate the locations of MUs, discussed in [7]. GPR is a generic supervised learning method designed to solve regression and probabilistic classification problems. Under this method, an unknown nonlinear function is assumed to be random, and to follow a Gaussian Process (GP). In contrast to kNN and SVM, GPR is able to provide probabilistic output, for example, the posterior distribution of

the MU position, after given an online measurement and a set of fingerprints with RSS vectors. Besides, without LoS and NLoS identification, this machine learning approximation method can efficiently identify MUs positions after training with limited reference users, and it significantly decreases the computational complexity as well.

B. Our Approach and Contributions

In this paper, we propose a novel positioning technique, called Beamforming-based Machine Learning for Positioning (*BeamMaP*) to meet the above challenges. *BeamMaP* employs a machine learning regression technique based on the efficient beamforming transmission patterns in order to estimate the location of MUs. *BeamMaP* can instantaneously predict the locations of MUs after generating the Machine Learning (ML) regression network model and help the base stations to distribute beams in an efficient way. Moreover, *BeamMaP* can implement the real-time detection to update the input data sets including LoS and NLoS multipath channels.
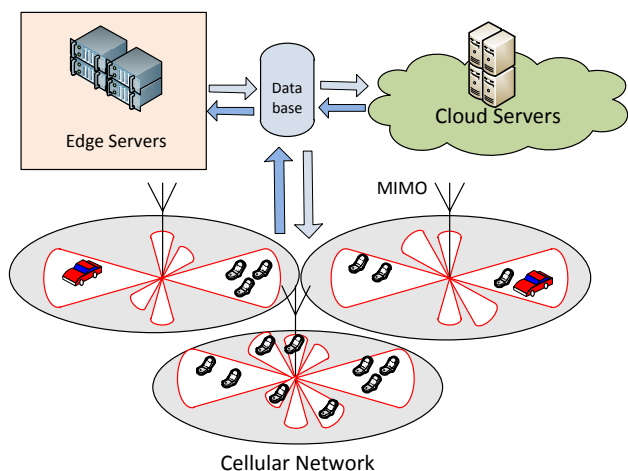
Figure 1. BeamMap positioning system in cellular networks.

The *BeamMaP* design is illustrated in Figure 1. The beamforming system in each BS installed massive MIMO antennas serves more than one MU. When a MU transmits on the uplink, we can obtain a vector of RSS (or a fingerprint) comprising LoS and NLoS multipaths measured by the massive antennas array in the BS. The detected uplink signals or RSS information are collected and submitted to the edge servers or cloud servers for calculation. Then the adaptive array systems can formulate a single or more beams with different weights to different directions according to the demands of MUs. Furthermore, MUs can process signals from a single MIMO base station, provided the BS and users were synchronized, which can be easily implemented by a two-way protocol by adding some additional overheads [13]. Besides, in order to avoid the pilot contamination occurred in massive MIMO system between cells, some reuse pilot schemes and particular modulation technology, such as Orthogonal Frequency-Division Multiplexing (OFDM) or Code-Division Multiple Access (CDMA) should be applied in our system [14]. Furthermore, massive MIMO systems combined with beamforming antenna technologies are considered to play a key role in the next generation wireless communication systems [15]. Optimal

beamforming techniques, such as adaptive beamforming, are mentioned to be employed in localization and provide energy saving of the MIMO systems. *BeamMaP* employs adaptive beamforming as a candidate in building the testing process. Compared with switched beamforming, adaptive beamforming can cover a larger area of MUs when the number of beams and bandwidths range shared are the same, and it also offers more comprehensive interference rejection [15]. Therefore, *BeamMaP* not only can improve the efficiency of coverage for users, but can also result in significant reduction in energy consumption of base stations.

The following contributions are made in this paper:

- We employ a supervised machine learning regression approach to accurately locate the MUs in a single cellular system.

- We present extensive performance results from simulations exploring the effects of various componential parameters.

- We prove our proposed machine learning method is more efficiency and steady in the positioning system compared with kNN and SVM.

- We use an adaptive beamforming method to build the testing users model to increase the efficiency of the ML model.

The rest of this paper is organized as follows: Section II presents the *BeamMaP* positioning system design, including the input data sets collected for training, the machine learning model and testing process. In Section III, we present performance evaluation results to analyze the impact factors. Section IV presents our conclusions.

II. BEAMMAP POSITIONING SYSTEM DESIGN

Driven by the above motivations, the *BeamMaP* framework is illustrated in Figure 2.

We firstly need to collect the fingerprints (RSS vectors) to generate the training data sets. Due to the unknown directions of MUs, we assume the beams weights in a uniform distribution trying to cover more MUs in comparison with the random distribution in the beginning status. Then, *BeamMaP* starts to explore the GPR method to train the collected raw data arrays, which include the RSSs of LoS and NLoS in the scenario. Some parameters set up in the ML regression model are able to be estimated in the training process. Furthermore, in order to avoid the overfitting in the training process, we follow the K^*-fold cross-validation to partition a sample of input data sets into complementary subsets, performing one subset as the training set (the orange blocks in the figure), and validating the analysis on the other subset as the testing set (the blue blocks in the figure). Multiple rounds of cross-validation are performed using different partitions, and the validation results are combined (e.g., averaged) over the rounds to give an estimate of the model's predictive performance. Moreover, we choose the Root-Mean-Square Estimation Error (RMSE) as the metric, which will be introduced in the experiment section. We set up a threshold σ to analyze the training process of the ML model. If the RMSE in the model is larger than σ, it will back up to the beginning of the ML process, requiring that
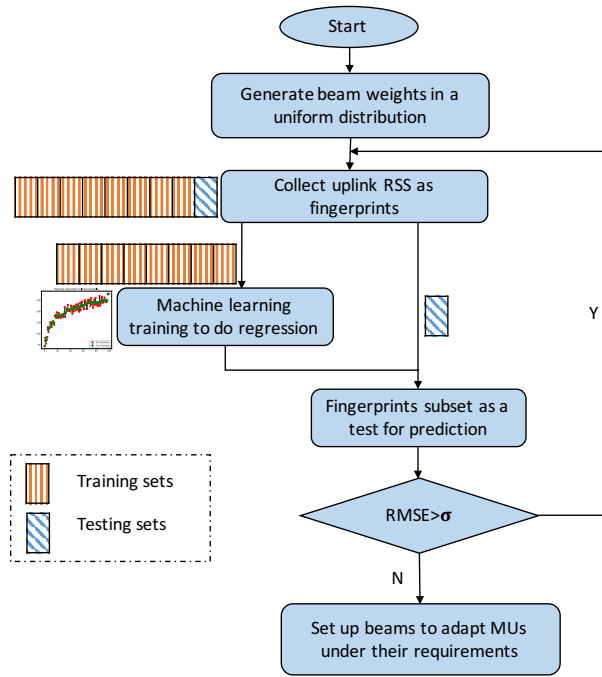
Figure 2. BeamMap's positioning system framework (adaptive σ chosen)

TABLE I. BASIC NOTATIONS REPRESENTATIVE.

Notation	Corresponding meaning
K, k	the number of antennas in BS, antenna index
M, m	the number of MUs, MU index
ρ	the transmission power of each mobile user
S	the number of training reference MUs
s_m	the symbol vector transmitted by the mth mobile user,
$\mathbf{s}$	the sum symbol vectors transmitted by all MUs
r_k	the received symbol vector at the kth antenna in BS,
$\mathbf{r}$	the sum signal strength vectors in BS
$h_{k,m}$	fading uplink channel between mth MU and kth antenna ,
$\mathbf{H}$	the uplink channel matrix between all MUs and BS antennas
$\alpha_{k,m}$	small-scale fading coefficient between mth MU and kth antenna ,
$q_{k,m}$	large-scale fading coefficient between mth MU and kth antenna
n_k	the additive white Gaussian noise vector received in the antenna k
$\mathbf{n}$	the sum additive white Gaussian noise vectors in the BS
$p_{k,m}$	RSS of mth MU at kth antenna in BS
$\mathbf{p}_m$	uplink RSS vectors of MU in all antennas of BS
n	the Path Loss Exponent (PLE) for LoS or NLoS channel
σ_s	the shadow fading in dB
$\widetilde{\mathbf{p}}_a$	the uplink RSS vector for the ath training MU
$\widetilde{\mathbf{P}}$	the training data matrix for S coordinates of MUs chosen
$\widehat{\mathbf{p}}_m$	the uplink RSS vector of the mth testing MU
$(\widehat{\mathbf{x}}_m, \widehat{\mathbf{y}}_m)$	the coordinate of the mth testing user in vector $(\widehat{\mathbf{x}}, \widehat{\mathbf{y}})$
$(\widetilde{\mathbf{x}}_m, \widetilde{\mathbf{y}}_m)$	the coordinate of the mth training user in vector $(\widetilde{\mathbf{x}}, \widetilde{\mathbf{y}})$
$[\mu^x]_m$	the estimation value of the mth testing user $\widehat{\mathbf{x}}_m$-coordinate
$[\sigma^x]_m$	the variance for errors of user $\widehat{\mathbf{x}}_m$-coordinate

the ML process continue the training process. If the RMSE is less than or equal to σ, the parameters in the model have been generated successfully in the estimation, and we should adjust the system to set up beams to cover the mobile users under their requirements. The detailed model is designed in the following part.

A. Input Data Sets for Training – Uplink Transmission in 5G MIMO Model

In this section, we build a wireless network model to locate Mobile Users (MUs) in a single cellular 5G network system. We assume one Base Station (BS) with K ($K \geqslant M$) antennas to serve M single-antenna MUs in the cell. We consider MUs simultaneously transmit M symbols, $\mathbf{s} = (s_1, ..., s_M)^T$, the massive MIMO antennas array in the base station can receive the sum signal strength vectors $\mathbf{r} = (r_1, ..., r_K)^T$:

$$\mathbf{r} = \sqrt{\rho}\mathbf{H}\mathbf{s} + \mathbf{n} \qquad (1)$$

Here ρ is a constant denoting the transmission power of each mobile user; $\mathbf{H}$ is the $K \times M$ channel matrix, with $h_{k,m} = \alpha_{k,m}\sqrt{q_{k,m}}, \forall k = 1, ..., K$ and $m = 1, ..., M$ as the transmission channel element for mth mobile user uplink to the kth antenna in the base station. $\alpha_{k,m}$ and $q_{k,m}$ are respectively the small-scale and large-scale fading coefficients. The large-scale fading $q_{k,m}$ (related to shadowing noise variance) is assumed to be a constant in the urban or suburban environment, and the small-scale fading $\alpha_{k,m}$ is considered to be an independent and identically distributed complex Gaussian distribution (Rayleigh distribution), with $\alpha_{k,m} \sim \mathcal{CN}(0,1)$. In addition, $\mathbf{n} = (n_1, ..., n_K)^T$ represents the additive white Gaussian noise vector given by $n_k \sim \mathcal{N}(0,1)$. We list the basic notations in Table I.

From (1), we are considering the sum signal strength vectors from all users to antennas. In order to separate the

multiple users RSS in $\mathbf{r}$, we have different schemes to extract the kth user RSS r_k. In order to capture the effective signals, the pilot signal vector s_k should be modulated as mutually orthogonal during transmission so that it can satisfy $s_i^H \cdot s_j = 0$ ($i \neq j$) [14]. Particular modulation techniques, such as OFDM or orthogonal CDMA employed as the coded schemes in the transmission systems. Minimum Mean Square Error (MMSE) being an appropriate solution, we can simply extract each user signal strength from the combination signals of all MUs and then distinguish the signals and noise by setting a threshold in the receiving part.

$$\mathbf{s}^H\mathbf{r} = \sqrt{\rho}\mathbf{H} + \mathbf{s}^H\mathbf{n} \qquad (2)$$

Taken all assumptions into account, we can acquire the single user's RSS as $p_{k,m}$ in:

$$p_{k,m} = \left\| s_m^H r_k \right\|^2 = \rho \left| h_{k,m} \right|^2 = \rho\alpha_{k,m}^2 \left| q_{k,m} \right| \qquad (3)$$

Also, we accumulate all MU uplink power vectors from all antennas in BS: $\mathbf{p}_m = [p_{1,m}^{\text{dB}}, p_{2,m}^{\text{dB}}, ..., p_{K,m}^{\text{dB}}]$. Established on the received power model, we can acquire the power data sets by converting (3) to the log distance path-loss model but they are limited in the lower frequency and small cellular environment [16]. Additionally, through our experiment, we observe the COST Hata model (COST is a radio propagation model that extends the urban Hata model to cover a more elaborate range of frequencies, which is developed by a European Union Forum for cooperative scientific research) also cannot adapt the different higher frequency 5G network system, even though it is popularly employed in the urban cellular network [17]. Also, the path loss models currently employed in the 3GPP 3D model is the ABG model form but without a frequency dependent parameter and additional dependencies on base station or terminal height, and only used in LoS scenario [18]. Therefore, we are considering to employ the Close-in (CI) free space reference distance Path Loss (PL)

model, which is noted multi-frequency and covers the 0.5-100 GHz band [18]. The CI-PL model is also transferred from (3) to adapt LoS and NLoS realistic scenarios through adding the free space path loss and optimizing the parameters:

$$P_{loss}(f_c, d)[\text{dB}] = \text{FS}(f_c, 1\text{m}) + 10n\log_{10}(\frac{d}{1\text{m}}) + \sigma_s \quad (4)$$

Here f_c is the carrier frequency in Hz, n is the Path Loss Exponent (PLE) describing the attenuation of a signal passing through a channel, d is the distance between MU and each antenna in BS and σ_s is the shadow fading in dB. The Free Space Path Loss (FS) in (4) is standardized to a reference distance of 1 m. FS with frequency f_c is given by:

$$\text{FS}(f_c, 1\text{m}) = 20\log_{10}(\frac{4\pi f_c}{\nu}) \quad (5)$$

In (5), ν denotes the speed of light. The CI-PL model is represented as the relationship between propagation path loss and TX-RX distance based on a straight line drawn on a two-Dimensional (2D) map, passing through obstructions, and used in both LoS and NLoS environment. While we are considering CI-PL in the urban cellular network of 5G system model, the parameters are measured as $n = 2.0, \sigma_s = 4.1\text{dB}$ in LoS and $n = 3.0, \sigma_s = 6.8\text{dB}$ in NLoS using omnidirectional antennas [18]. Due to the same transmission power assumed for each MU, we can use the CI-PL model as the RSS parameters to acquire the training data sets.

Additionally, for each MU's uplink transmission, multi-paths signals can be received by multiple antennas, some of them are LoS and the others are NLoS responses. So we consider the LoS probability model in the current 3GPP/ITU model in the MIMO receiving part when setting up the training data. It means the uplink response array of MIMO antenna includes LoS and NLoS components for each MU. From [18], in terms of Mean Squared Error (MSE) between the LoS probability from the data and the models, we choose the d_1/d_2 model as follows:

$$p(d) = \min(\frac{d_1}{d_2}, 1)(1 - e^{-\frac{d}{d_2}}) + e^{-\frac{d}{d_2}} \quad (6)$$

where d is the 2D distance between MU and antennas in meters and d_1, d_2 can be optimized to fit a scenario of parameters (we choose $d_1 = 20$, $d_2 = 39$ because it acquires minimum MSE in adapting the urban scenario).

B. Machine Learning Model

Given the RSS vector $\mathbf{p}_m = [p_{1,m}^{\text{dB}}, p_{2,m}^{\text{dB}}, ..., p_{K,m}^{\text{dB}}]$, our goal is to find the position of the mth MU in the two dimensional plane, denoted by (x_m, y_m). We build the functions $f_x(.)$ and $f_y(.)$ which take the uplink RSS vector $\mathbf{p}_m$ of a given user m as input and provide the user's location coordinates (x_m, y_m) as output, and try to learn as follows:

$$x_m = f_x(\mathbf{p}_m) \quad \text{and} \quad y_m = f_y(\mathbf{p}_m), \forall x_m, y_m \quad (7)$$

Derived from CI-PL model for the input training model, the learning functions can be classified as a nonlinear regression problem. We follow GPR as a supervised machine learning approach, with a training phase and a test phase, to learn $f_x(\mathbf{p}_m)$ and $f_y(\mathbf{p}_m)$. In the training level, we consider RSS vector $\mathbf{p}_m$ derived from the CI-PL model in both LoS and NLoS conditions. Prior to it, we need to acquire the antennas coordinates, the training users coordinates, and some other parameters. In the testing phase, the RSS vectors of the testing users will be chosen distributed according to a Rice distribution to satisfy the adaptive beamforming pattern, whose location coordinates are unknown.

C. Training and Beamforming-based Prediction Phase

GPR uses the kernel function to define the covariance over the objective functions and uses the observed training data to define a likelihood function. Gaussian processes are parameterized by a mean function μ_x and covariance function $\mathbf{K}(\mathbf{p}_i, \mathbf{p}_j)$, which means $f_x(.), f_y(.) \sim \mathcal{N}(\mu, \sigma^2)$. Usually the mean matrix function is equal to 0, and the covariance matrix function, also known as kernel matrix function, is used to model the correlation between output samples as a function of the input samples. The kernel matrix function $\mathbf{K}(.,.)$ contains $k(\mathbf{p}_i, \mathbf{p}_j), \forall i, j = 1, ..., M$ as the entries to define the relationship between the RSS of the users. We usually use a weighted-sum of squared exponential and linear functions, which servers the stationary component and non-stationary component respectively, to generate the regression function:

$$k(\mathbf{p}_i, \mathbf{p}_j) = \upsilon_0 e^{-\frac{1}{2}\mathbf{A}\|\mathbf{p}_i - \mathbf{p}_j\|^2} + \nu_1 \mathbf{p}_i^T \mathbf{p}_j \quad (8)$$

Here $\mathbf{A} = \mathbf{diag}(\eta_k), \forall k = 1, ...K$. It will cover the LoS and NLoS matching with each MU. So the parameters vector $\Lambda = [\upsilon_0, \mathbf{A}, \upsilon_1] = [\upsilon_0, \eta_1..., \eta_K, \upsilon_1]$ can be estimated from the training data. In order to learn the target vector $\overline{\Lambda}$, we choose S coordinates of MUs as the training data matrix $\widetilde{\mathbf{P}}$ denoted $\widetilde{\mathbf{P}} = [\widetilde{\mathbf{p}_1}, \widetilde{\mathbf{p}_2}...\widetilde{\mathbf{p}_S}]$ and use the maximum-likelihood method to predict the $(\widetilde{x}, \widetilde{y})$-coordinates. According to the property of a Gaussian process, we can acquire the learned vector $\overline{\Lambda}$ by employing the maximum-likelihood of the $S \times 1$ training $\widetilde{\mathbf{x}}$-coordinate vector:

$$\overline{\Lambda} = \underset{\Lambda}{\text{argmax}} \log(p(\widetilde{\mathbf{x}}|\widetilde{\mathbf{P}}, \Lambda)) \sim N(\widetilde{\mathbf{x}}; 0, \widetilde{\mathbf{K}}) \quad (9)$$

The parameter vector follows as GP, which is a non-convex function as shown in the [7], and can not be solved well in the training process. Several methods introduced in [19], such as stochastic gradient descent, mini-batching or momentum, can help to solve the non-convex problem. Established on the ML method in the training problem, we decided to employ stochastic gradient descent method [19] to obtain the optimum vector $\overline{\Lambda}$ in convergence to a local maximum.

In the prediction phase, the predictive distribution $p(\widehat{\mathbf{x}}_m|\widetilde{\mathbf{P}}, \widetilde{\mathbf{x}}, \widehat{\mathbf{p}}_m)$ in terms of posteriori density function, is applied as estimation of the testing user $\widehat{\mathbf{x}}_m$-coordinate, which also follows the Gaussian distribution with mean $[\mu^x]_m$ and variance $[\sigma^x]_m$, $\widehat{\mathbf{x}}_m|\widetilde{\mathbf{P}}, \widetilde{\mathbf{x}}, \widehat{\mathbf{p}}_m \sim \mathcal{N}([\mu^x]_m, [\sigma^x]_m)$:

$$[\mu^x]_m = \sum_{a=1}^{S} k(\widehat{\mathbf{p}}_m, \widetilde{\mathbf{p}}_a)[\widetilde{\mathbf{K}}^{-1}\widetilde{\mathbf{x}}]_a,$$

$$[\sigma^x]_m = k(\widehat{\mathbf{p}}_m, \widehat{\mathbf{p}}_m) - \sum_{a=1}^{S}\sum_{b=1}^{S} k(\widehat{\mathbf{p}}_m, \widetilde{\mathbf{p}}_a)[\widetilde{\mathbf{K}}^{-1}]_{ab} \cdot k(\widetilde{\mathbf{p}}_b, \widehat{\mathbf{p}}_m)$$

$$(10)$$

where the mean $[\mu^x]_m$ indicates the estimation value of test user $\widehat{\mathrm{x}}_m$-coordinate and the variance $[\sigma^x]_m$ represents the variance for errors of user $\widehat{\mathrm{x}}_m$-coordinate. $\widehat{\mathbf{p}}_m$ denotes the received power vector of the mth testing MU, and $\widetilde{\mathbf{p}}_a$ denotes the ath power vector in the received training power matrix $\widehat{\mathbf{P}}$. For the computational complexity of GPR, we observe from (10), $[\mu^x]_m$ needs to sum up S operations for $\widetilde{\mathbf{K}}^{-1}\widetilde{\mathbf{x}}$, which requires $\mathcal{O}(S^2)$. In total, $[\mu^x]_m$ incurs a time complexity of $\mathcal{O}(S^3)$.

Subsequently, we choose the locations of test MUs based on the beamforming pattern. Beams can be optimized to distribute and spread with the demand users. In the real scenarios, some hot spot areas need large bandwidth and some other areas only need small bandwidth to satisfy with few mobile users. The locations of MUs always follow a Rice distribution. Therefore, the coordinates of test users in positions prediction can be chosen from input fingerprints following a Rice distribution, which will satisfy with the beams distribution in an adaptive way. *BeamMaP* being as a prediction assistant, it will cooperate with a better beamforming scheme to distribute the bandwidths in efficiency. During the experiments, we will compare with switched beamforming patterns which beams are distributed uniformly in the system. Furthermore, we employ the same proposed regression method to estimate the $\widehat{\mathrm{y}}_m$-coordinate of test user. Also, we can acquire the mean $[\mu^y]_m$ and variance $[\sigma^y]_m$ as the predictive parameters.

III. PERFORMANCE EVALUATION

In this section, we conduct simulations to evaluate the performance of *BeamMaP* as the machine learning method in estimating the locations of testing MUs. In order to simulate a realistic environment, we set up the parameters of path loss model based on the 5G 3GPP/ITU Micro-Urban model [18].

TABLE II. PARAMETERS FOR SIMULATION.

Description	Value
Path loss parameters (5G 3GPP/ITU Micro-Urban model [18])	$n = 2.0, \sigma_s = 4.1$dB for LoS, $n = 3.0, \sigma_s = 6.8$dB for NLoS, $d_1 = 20, d_2 = 39$
Modulation Scheme	OFDM (Orthogonal CDMA)
MU transmit power	23 dBm (200 mW)
Minimum SNR for channel estimation	1 dBm
Number of antennas in BS	64(8×8),100(10×10),144 (12×12)
Maximum number of training fingerprints	90000
Number of testing MUs	100
The space between antennas	0.12, 0.3, 0.48 m
The space between training MUs	1 m
Threshold to control the training process (σ)	[5, 35] m

A. Parameters Set Up

The parameters used in the simulation are shown in Table II. According to the analysis of different environment in Section II-A, the path loss parameters n and σ_s are chosen for adapting the crowded urban area. The MU transmit power is chosen as per LTE standards to be 23 dBm [20]. In practice testing, the minimum SNR required is determined by the normalized mean squared error of the channel estimates [18]. For our simulations, we set the minimum required SNR to 1 dB. Considering that currently the number of MIMO antennas of the BS can be designed from 64 to 156, we

assume $K = 64, 100, 144$ antennas uniformly distributed as a 8×8, 10×10 and 12×12 squares. We assume that the MIMO antennas are installed at the center of a cellular network which can distribute the beams in each direction with the same maximum reach. Figure 3 shows an example of the deployment of the base station antennas and the surrounding reference MUs consisting of a squared antennas array with 16 antennas covering $x \in [5, 30]$ and $y \in [10, 70]$ area (meters in unit). The fingerprints for MUs are distributed in a grid covering dimensions $x \in [50, 130]$ and $y \in [20, 140]$. We split the fingerprints into a training part and a testing part, then follow the K^*-fold cross-validation method (i.e., $K^* = 10$) to do the regression and average the result over several runs.
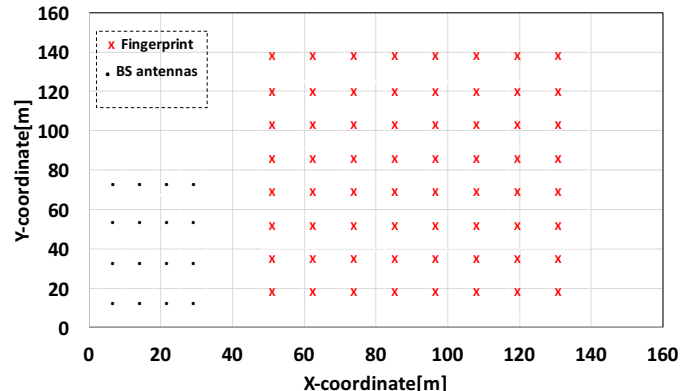
Figure 3. The deployment example of MIMO antennas (BS antennas) and reference MUs (Fingerprint)

The coordinates of MUs and antennas are selected as positive values in the simulation. In order to reduce the interference between the uplink received signals in the massive MIMO, the spacing between antennas can be selected from 0.12 to 0.5 m, which is based on the function of the OFDM signal wavelength [21]. If without considering the influence of the other parameters, we assume the space between antennas be 0.5 m to better differentiate the RSS vectors in the simulation. In addition, we choose $S = 90000$ as the maximum number of fingerprints with 1 meter spacing between MUs in a grid covering about 300 m $\times$ 300 m, which covers 95% of LoS components in the single cellular system. In practice, for example, we can install a cellular BS with a 12×12 square antennas on the top roof of our engineering building located in Washington DC of United States. Each antenna equipped with one transceiver can receive and/or send the signals from and/or to each MU. The coordinates of references MUs will be chosen in a grid around the building, the spaces between MUs are set up as 1 meter. We can use a moving MU in each chosen locations to send the signals to all the receivers in BS each time. The computers as a RSS reader in BS will calculate each RSS vector from the signals of the reference MUs and accumulate all the uplink RSSs as the training data sets. Due to lack of hardware support, the RSS vector $\mathbf{p}_m$ for each MU in antennas is generated from the CI-PL model in (4) and (5), which is proved in the Aalborg, Denmark environment [18].

Meanwhile, each antenna in MIMO can receive LoS or NLoS from the different direction. In order to model the real-life scenario including LoS and NLoS, the RSS matrix $\widetilde{\mathbf{P}}$ as the fingerprints collected from all antennas follows the

LoS and NLoS distribution in (6). We calculate them through generating a probability function in the simulation. During the training phase, while we are learning the parameter vector $\overline{\Lambda}$, we run the training locations on randomly choosing the start points, so as to avoid the convergence to a bad optimal solution. We assume the threshold $\sigma \in [5, 35]$ m, which needs to be feasibly chosen depending on the different training data sets to fit in the experiment. In the testing phase, we choose the Rice distribution of 100 testing users from RSS vectors in fingerprints to efficiently steer beams in a flexible way. The Rice distribution is selected as $R \sim \text{Rice}(50, 1)$ through experiments because of the maximum coverage of a single cell network and variance of spacing in 1 m.

B. Performance on Metrics

After RMSE is reaching less than σ, we test the accuracy of the simulation model in using the linear sampling coordinates, which are convenient to observe. For example, we use a 12 $\times$ 12 antenna array located in $x \in [40, 46]$ and $y \in [100, 106]$ area as reference locations. In order to observe the tracking locations in a 'linear' status, we initialize to employ a linear log-function ($y = 50\log x$) to sample the positions of 100 testing mobile users from fingerprints. We can then track the MUs and compare with their true positions, as shown in Figure 4. It is simple to find the estimated position of testing users not far from the linear true positions 'line', where the interval between them can not exceed 8.5 m. Due to the limitation of test users and sampling, we are not able to decide other impact factors for the accuracy of estimation.
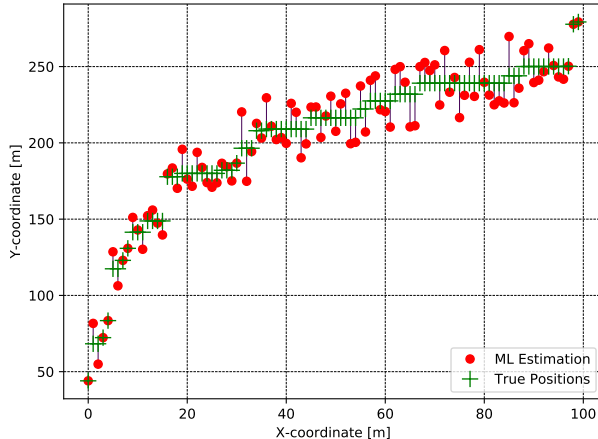
Figure 4. Position estimation in a linear distribution of Testing MUs

Furthermore, we use the Root-Mean-Squared Estimation Error (RMSE) as the metric to analyze the performance of the estimation methods. RMSE is formulated as:

$$\text{RMSE} = \sqrt{\frac{\sum_{m=1}^{\widehat{M}} (\widehat{x}_m - [\mu^x]_m)^2 + (\widehat{y}_m - [\mu^y]_m)^2}{\widehat{M}}} \quad (11)$$

where $[\mu^x]_m$ and $[\mu^y]_m$ are the estimation of test user's coordinates $\widehat{x}_m$ and $\widehat{y}_m$, respectively. $\widehat{M}$ is the number of testing MUs. We limit the analysis to the RMSE metric.

In Figure 5, we are trying to determine the influence of training samples for different number of antennas in the base

station. As the antennas are installed in a fixed space, some of them will receive the LoS signals and others will receive the NLoS signals. The distribution between LoS and NLoS follows the probability function of LoS in (6), as assumed previously. We show 95% confidence intervals from 30 trials for each data point. As observed from Figure 5, we know when the sampling in training locations increases, the RMSE keeps decreasing with fixed antennas size, which means acquiring the higher the accuracy of estimation. When the sampling is the same, more LoS signals will be received in the large size antenna array, which will help to decrease the interference, while fewer NLoS signals will be identified as LoS in the receiver. For example, RMSE in 12×12 antennas is almost half of 8 × 8 in the same sampling condition. Also, the higher dimension of fingerprints for training will acquire more accuracy estimation in the terms of the increase number of antennas.
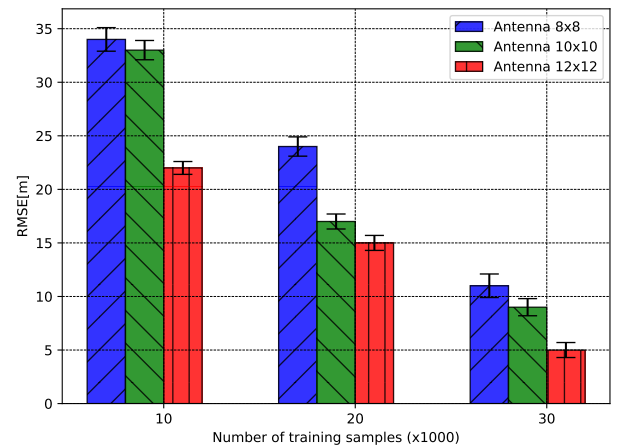
Figure 5. RMSE vs. number of training samples for different size of antennas array

In order to know the effect of antenna size in a MIMO system, we change the spacing between antennas as in Figure 6. The RMSE for different spacing but the same number of antennas shows no significant change. When the space is changed from 0.12 m to 0.30 m, the differential in RMSE for 8 × 8, 10 × 10 and 12 × 12 antennas is 5 m on average. However, comparing the spacing in 0.12 m and 0.48 m, the RMSE is dramatically decreased, caused by the ability of identification between LoS and NLoS, and the size of sampling.

We compare the running time performance and RMSE metric of different machine learning approaches (*BeamMaP*, kNN and SVM) in the dynamic environments. The shadowing noises for LoS and NLoS are set up to change from 1 dB to 4 dB, which can be regarded as different scenarios in practice. The same training data sets are generated through CI-PI model. We run the simulations simultaneously on the three same workstations (Ubuntu 16.04 LTS system on 3.6GHZ Intel Core i7-4790 CPU with eight cores). The results are shown in Table III. In general, with the increase of shadowing noise, the RMSE (in meters) for all approaches gradually becomes larger. Compared with kNN and SVM, RMSE for the proposed *BeamMaP* is obviously smaller. Although the training time for kNN is much less than *BeamMaP* and SVM, the testing time for our proposed is averaged as 0.35 s which is far less than the
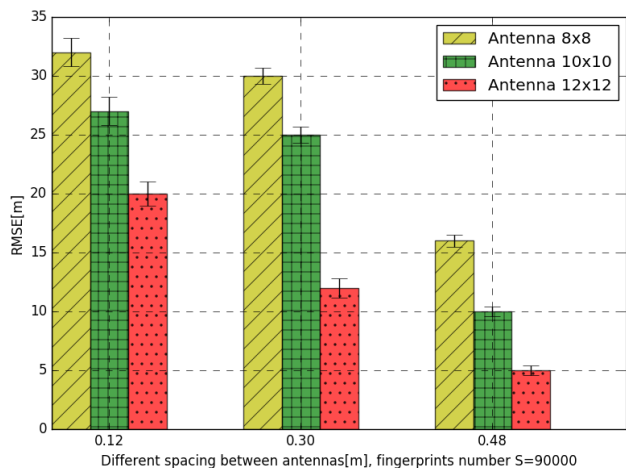
Figure 6. RMSE vs. different spacing between antennas for different size of antennas array

others. The testing time is calculated from 100 testing samples in average.

TABLE III. COMPARISON BETWEEN DIFFERENT APPROACHES.

Shadowing Noise	BeamMap	kNN	SVM
	RMSE[m]		
1 dB	3.5	8.5	10.2
2 dB	8.4	13.2	15.5
3 dB	15.6	20.2	20.4
4 dB	22.3	27.4	30.8
Phase	Running time		
Training	20.30 hours	8 hours	21 hours
Testing	0.35 s	1.20 s	0.874 s

kNN being as a unsupervised method, is served as positioning the target MU through collecting and analyzing the closest k reference neighbors. The time complexity known as $\mathcal{O}(KS + kS)$ is depended on the S cardinality of the training data set and the K (the number of antennas) dimension of each sample [11]. Despite SVM is mostly used in the linear condition, our nonlinear problem needs to be transferred into the quadratic problem directly, which involves inverting the kernel matrix. It has complexity on the order of $\mathcal{O}(S^3)$ same with our proposed model. The estimation of this method is based on a subset of the training samples (known as support vectors). However, these two models can only choose LoS signals in the RSS vector of training data sets, the NLoS elements have to be removed and become 0. The imbalance of the training data sets (no distinguishment between LoS and NLoS in the vectors) will degrade the performance of kNN and SVM. The original data sets can influence the RMSE which reaches two times larger than recent simulation. For example, while the shadowing noise is 2 dB, the RMSE for kNN and SVM will become 25 and 30 m. Therefore, the shortest testing time spent and smallest RMSE in the simulation will prove that our proposed model is steadier and better optimized in the much noisy or highly cluttered multipath scenarios; also the gap of the training time between them can be shortened in the future advanced hardware.

Furthermore, even though we choose the testing users from fingerprints in Rice distribution for the estimation process, the adaptive beamforming pattern in BS appears not to be

necessary in the machine learning localization. In order to compare adaptive beamforming with switched beamforming, we assume the number of antennas as 12×12 to maximize the sampling ratio. During the testing phase, we model the switched beamforming as a uniform distribution with the same mean and variance as the Rice distribution in adaptive beamforming. In Figure 7, we conclude that adaptive beamforming or Rice distribution in the regression system plays a better role, it only can reach the half of RMSE compared with uniform distribution with the same sampling training index.
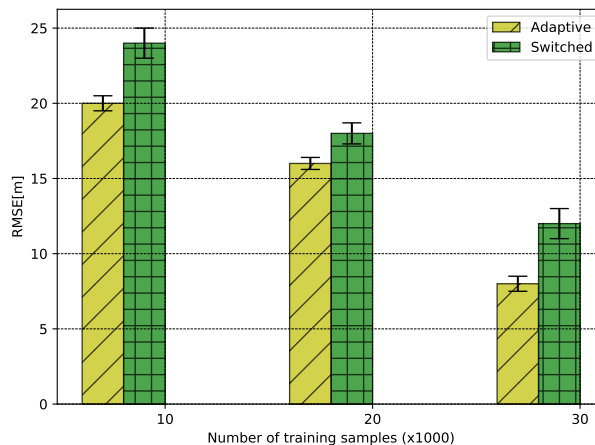
Figure 7. RMSE vs. number of samples for different beamforming patterns

More efficiency for adaptive beamforming is achieved by randomly selecting the testing users similar to Monte-Carlo sampling. The reason is that more testing users are gathered together in one direction for the adaptive pattern, but testing users in uniform distribution (switched pattern) are separately localized, which will accumulate the estimation errors and lead to the increase of RMSE. In addition, the slow offline machine learning process can help to speed up the distribution of bandwidth in adaptive beamforming after employing the faster online testing system. The testing process only needs less than 0.35 s.

IV. CONCLUSION AND FUTURE WORKS

In this paper, we present a *BeamMaP* positioning method, combined with a supervised machine learning approach and an online adaptive beamforming testing process, to estimate the position of mobile users. *BeamMaP* can estimate the location of the MUs within 5 meters deviation, which is much better than some conventional methods like GPS and also is sufficient for beam signals to cover the channels between MU and BS. Numerical results show the accuracy of positioning, as determined by the size of sampling, the dimension of antennas, their quantity and distance, and the number of received LoS and NLoS signals. In comparison with kNN and SVM, our proposed machine learning method is proved more efficiency and steadier for positioning in highly cluttered multipath system. Furthermore, we conclude that the adaptive beamforming pattern can increase the accuracy and efficiency of position estimation in comparison with switched beamforming. However, the RSS fingerprinting methods may fail in changeable environments (e.g., rainy or windy weather)

due to the long online training time, and more training data sets in different dimensions should be collected to increase the adaption of positioning system. Moreover, some deep learning or hybrid machine learning methods can be explored and make some improvements in the future research.

REFERENCES

[1] C. Liu, M. Xu, and S. Subramaniam, "A reconfigurable high-performance optical data center architecture," in 2016 IEEE Global Communications Conference (GLOBECOM). IEEE, 2016, pp. 1–6.

[2] M. Xu, C. Liu, and S. Subramaniam, "Podca: A passive optical data center network architecture," Journal of Optical Communications and Networking, vol. 10, no. 4, 2018, pp. 409–420.

[3] M. S. Leeson, "Introductory chapter: The future of mobile communications," in The Fifth Generation (5G) of Wireless Communication. IntechOpen, 2019.

[4] S. K. Routray, P. Mishra, S. Sarkar, A. Javali, and S. Ramnath, "Communication bandwidth for emerging networks: Trends and prospects," arXiv preprint arXiv:1903.04811, 2019.

[5] F. Boccardi, R. W. Heath, A. Lozano, T. L. Marzetta, and P. Popovski, "Five disruptive technology directions for 5G," IEEE Communications Magazine, vol. 52, no. 2, 2014, pp. 74–80.

[6] L. Lu, G. Y. Li, A. L. Swindlehurst, A. Ashikhmin, and R. Zhang, "An overview of massive MIMO: Benefits and challenges," IEEE journal of selected topics in signal processing, vol. 8, no. 5, 2014, pp. 742–758.

[7] S. Kumar, R. M. Hegde, and N. Trigoni, "Gaussian process regression for fingerprinting based localization," Ad Hoc Networks, vol. 51, 2016, pp. 1–10.

[8] N. Garcia, H. Wymeersch, E. G. Larsson, A. M. Haimovich, and M. Coulon, "Direct localization for massive MIMO," IEEE Transactions on Signal Processing, vol. 65, no. 10, 2017, pp. 2475–2487.

[9] J. Vieira, E. Leitinger, M. Sarajlic, X. Li, and F. Tufvesson, "Deep convolutional neural networks for massive MIMO fingerprint-based positioning," arXiv preprint arXiv:1708.06235, 2017.

[10] B. Hofmann-Wellenhof, H. Lichtenegger, and J. Collins, Global positioning system: theory and practice. Springer Science & Business Media, 2012.

[11] L. M. Ni, Y. Liu, Y. C. Lau, and A. P. Patil, "LANDMARC: indoor location sensing using active RFID," Wireless networks, vol. 10, no. 6, 2004, pp. 701–710.

[12] M. Brunato and R. Battiti, "Statistical learning theory for location fingerprinting in wireless LANs," Computer Networks, vol. 47, no. 6, 2005, pp. 825–845.

[13] H. Wymeersch et al., "5G mm wave downlink vehicular positioning," in 2018 IEEE Global Communications Conference (GLOBECOM), 2018, pp. 206–212.

[14] A. Gorokhov, A. F. Naguib, A. Sutivong, D. A. Gore, and J. Tingfang, "Pilot signal transmission for an orthogonal frequency division wireless communication system," Oct. 4 2016, US Patent 9,461,859.

[15] E. Ali, M. Ismail, R. Nordin, and N. F. Abdulah, "Beamforming techniques for massive MIMO systems in 5G: overview, classification, and trends for future research," Frontiers of Information Technology & Electronic Engineering, vol. 18, no. 6, 2017, pp. 753–772.

[16] S. Jung, C. Lee, and D. Han, "Wi-Fi fingerprint-based approaches following log-distance path loss model for indoor positioning," in Intelligent Radio for Future Personal Terminals (IMWS-IRFPT), 2011 IEEE MTT-S International Microwave Workshop Series on. IEEE, 2011, pp. 1–2.

[17] M. Hata, "Empirical formula for propagation loss in land mobile radio services," IEEE transactions on Vehicular Technology, vol. 29, no. 3, 1980, pp. 317–325.

[18] K. Haneda et al., "5G 3GPP-like channel models for outdoor urban microcellular and macrocellular environments," in Vehicular Technology Conference (VTC Spring), 2016 IEEE 83rd. IEEE, 2016, pp. 1–7.

[19] P. Jain and P. Kar, "Non-convex optimization for machine learning," Foundations and Trends® in Machine Learning, vol. 10, no. 3-4, 2017, pp. 142–336.

[20] P. Joshi, D. Colombi, B. Thors, L.-E. Larsson, and C. Törnevik, "Output power levels of 4g user equipment and implications on realistic rf emf exposure assessments," IEEE Access, vol. 5, 2017, pp. 4545–4550.

[21] "Cisco 1250 dipole antenna spacing," 2019, available online: https://community.cisco.com/t5/other-wireless-mobility-subjects/specs-on-distance-between-antennas/td-p/1030478 [retrieved: May, 2019].